Compressed Radio Transmission of Spatial Field Measurements by Virtual Sensors

Reiner Jedermann, Henning Paul and Walter Lang

***Abstract*—The remote exploration or monitoring of an environment often includes sensor measurements at multiple probe points and reconstruction of the spatial distribution of the observed physical quantity by a regression model. Especially for long distances between the observer and the environment, required data volume for transmitting a parametric description of the spatial distribution becomes critical. Simple physical models or assumption of parametric base functions do not provide sufficient prediction accuracy. Statistically based methods for field reconstruction such as Kriging or Gaussian Process Regression provide good accuracy, even if the measurements are overlaid with noise, provided all sensor data is transmitted. The new method presented in this paper calculates a small set of quasi optimal virtual sensor positions located in-between the real sensors. By transmitting only the predicted values of these virtual sensors, the spatial field can be reconstructed with less transmitted data and without significantly increasing the prediction error. The new approach was verified in a simulation scenario for a temperature field caused by diffusion and advection phenomena, which yielded a data compression by a factor of up to four. For large variations of the number of sensors and of the magnitude of measurement noise, the prediction error was always lower compared with the parametric base function models.**

I. Introduction

Monitoring of the spatial distribution of a physical property in remote environments that are difficult to access for humans can be done by wireless systems, e.g., concentrations of a chemical pollutant in a lake [1], temperature and airflow in a chilled warehouse with nitrogen atmosphere [2], or geological or soil properties, e.g. soil moisture in large irrigation systems [3]. The typical information chain in these applications consists of the following elements:

See http://dx.doi.org/10.1109/WiSEE.2016.7877329 for official final version.

This research was supported by the German Research Foundation (DFG) for the project 'In-network data analysis of spatially distributed quantities' under grants Pa2507/1 and Je722/1. For further information, visit www.intelligentcontainer.com.

R. Jedermann is with the Institute for Microsensors, -actuators and -systems (email: rjedermann@imsas.uni-bremen.de).

H. Paul is with the Department of Communications Engineering (email: paul@ant.uni-bremen.de)

W. Lang is with the Microsystems Center Bremen (email: wlang@imsas.uni-bremen.de).

All three institutes are located at the University of Bremen, Germany

- The remote sensor system collects data at multiple probe points by a wireless sensor network or a mobile sensor or robot. The measurements are often overlaid with noise and local disturbances.
- A gateway collects the sensor data, pre-processes them, and sends them over a long-distance radio link to an observer.
- The observer carries out a field reconstruction by regression or interpolation techniques to predict the undisturbed, noise-free field values, for the probe locations as well as for points in-between.

Especially in extra-terrestrial applications, the required data volume that has to be transmitted over the radio link is a critical design issue, which should be reduced by adequate pre-processing on the gateway.

Parametric models have often been used to reduce data from spatial measurements to a small set of parameters by describing the spatial distribution by a sparse set of base functions. After estimating the parameters of these functions, the original measurement data can be discarded, resulting in a good compression rate. The base functions can be selected according to a physical model, e.g., a Green's function for diffusion processes [4], [5], [6], [7]. This Green's function is identical with the common Gaussian Radial Basis Functions (**RBF**) model [8], except for a time-dependent scaling factor.

Although these models provide good data compression, they introduce an additional error to the field reconstruction because real physical processes cannot be reduced to simple base functions. In almost any real application, diffusion processes are overlaid with other physical phenomena such as the transport of heat or chemicals by advection and convection or geological processes during rock and soil formation.

Non-parametric models are more flexible to approximate different shapes of the spatial field. These purely data-driven approaches take no assumptions of the underlying physical process or curve shape, except for some statistical properties.

Kriging [9], [10] and Gaussian Process Regression (**GPR**) [11], [12] provide a better fit to the data by estimating the field value as a linear combination of the measurements, but at the cost that the complete measurement data set is required for field reconstruction.

Smoothing splines are another important type of non-parametric models to represent the measurements of a wireless network [13]. They approximate the measurements by spline functions located at a dense network of knot positions. Due to

Please quote as: Jedermann, R.; Paul, H.; Lang, W.: Compressed radio transmission of spatial field measurements by virtual sensors. In: 2016 IEEE International Conference on Wireless for Space and Extreme Environments (WiSEE), Aachen, Germany, 2016, pp. 184-189. (doi: 10.1109/WiSEE.2016.7877329).

the high number of required knots, they have also limited capabilities for data compression.

In this paper we present a new approach that is based on the non-parametric Kriging model to achieve accurate field reconstruction, but also largely reduces the transmitted data volume over the radio link by representing the measurements by a small set of so called virtual sensors. The compressed description of the field consists of the location coordinates of the virtual sensors and the smoothed field values at their positions. The algorithm calculates quasi-optimal locations of these virtual sensors to minimize the prediction error compared to field reconstruction by the full data set. The term 'virtual sensors' has been mentioned in literature occasionally [14], but up to our knowledge, it has not been applied for data compression so far.

Other previous works [15] employ compression through random superposition of measurements to a smaller number of values transmitted on the cluster head communication links, but this approach requires centralized Compressed Sensing-based reconstruction.

In section 2 we shortly introduce the basic ideas behind the Kriging and RBF models, which serve as reference. Our new approach is described in section 3 with a focus on the strategy for setting the positions of the virtual sensors. The new method is compared with the reference models by simulation studies in terms of compression rate and prediction error in section 4.

II. Models for Spatial Field Reconstruction

For simplicity, we restrict the models to a two-dimensional field, but extension to three dimensions is straight forward.

We assume that the field $f(x,y)$ generated by a physical process is overlaid with Gaussian independent and identically distributed (i.i.d.) noise with RMS (Root mean square) σ_N. The prediction $g(x,y)$ of the model should be as close as possible to the true field values $f(x,y)$, which cannot be directly observed. The accuracy of the model and its capability to smooth the noise are evaluated by a quadratic error criterion (1), calculated for r_{Max} points, typically distributed on an equispaced grid.

$$\varepsilon_{\mathrm{Re}f} = \sqrt{\frac{1}{r_{Max}} \sum_{r=1}^{r_{\max}} \left(f(x_r, y_r) - g(x_r, y_r) \right)^2} \tag{1}$$

The estimation of the model has to be based on the sensor measurements m_s at s_{max} points at coordinates x_s and y_s, which serve as training data. During training, the following error criterion is minimized (2):

$$\varepsilon_T = \sqrt{\frac{1}{s_{Max}} \sum_{s=1}^{s_{\max}} \left(m_s - g(x_s, y_s) \right)^2} \tag{2}$$

The RBF model, for example, approximates the field with a sum of b_{Max} RBF functions with amplitudes a_i and widths λ_i at centers x_i, y_i and a constant offset c_0. In total, $4 \cdot b_{Max}+1$ parameters are required to describe the field.

$$g(x,y) = c_0 + \sum_{i=1}^{b_{\max}} a_i \cdot \exp\left(\frac{(x-x_i)^2 + (y-y_i)^2}{\lambda_i}\right) \tag{3}$$

Linear estimators such as Kriging and GPR predict the field by a weighted average of the measurements. The weighting factors ω_s depend on the coordinates of the target point at x,y (4). The number of sensor points used by the model is often restricted to the k_N closest neighboring sensors of the target point to avoid high computation loads.

$$g(x,y) = \sum_{s=1}^{k_N} \omega_s(x,y) \cdot m_s \tag{4}$$

The Kriging method calculates optimal values for the weighting factors ω_s, in order to minimize the expected squared prediction error for the related target point, under the condition that the observed values result from a second-order stationary spatial process, i.e., the mean $E\{m_i\}$ is independent of location, and the correlation of any two points i,k depends only on their distance $d_{i,k}$ according to the variogram function $\gamma(\cdot)$ in (5):

$$\gamma(d_{i,k}) = \frac{1}{2} E\left\{ \left(m_i - m_k \right)^2 \right\} \tag{5}$$

Ordinary Kriging additionally estimates $E\{m_i\}$. Calculation of the ω_i requires inversion of a matrix with order k_N+1. The matrix elements at i,k are set to $\gamma(d_{i,k})$ by the distances between the neighboring sensors points. The last row and column of the matrix are filled with ones, except for the last diagonal element, which is zero. More details can be found in earlier publications [9]. For anisotropic variogram functions, see statistical textbooks, such as [16].

The crucial step in applying the Kriging method is the estimation of the variogram by current or historic measurement data. The variogram estimation by experimental data has to be fitted by a conditionally negative definite model function. An example variogram model is given in section 3C.

The approach of GPR is similar to Kriging, except that it describes the spatial correlation between sensor points by a covariance matrix instead of a variogram model.

III. Virtual Sensors

Because the location of local field extrema is not known in advance, a high number of sensors are required to capture the spatial distribution of an unknown field. The basic idea of our approach is to identify a small set of sensor positions, which are able to capture the field without significant loss of accuracy. In case of mobile sensor nodes or measurement devices, most sensors can be switched off and only few of them can move to the identified optimal positions. In the

more general case of stationary sensors, virtual sensors can be simulated at the optimal positions. The virtual measurements at these positions are prediction by the regression model.

The field reconstruction by the observer is carried out in the same way as for the standard Kriging method, except that the weighted average in (4) is calculated for the virtual sensors instead of the real sensor positions. In the following, we name this new approach as '**Virtual Kriging**' in contrast to '**Full Kriging**' with all sensor positions.

This approach overcomes the disadvantage of the Full Kriging of requiring the transmission of all measurement data for field reconstruction. Instead only the locations x_v, y_v and the predicted values p_v at v_N virtual positions have to be transmitted, with total $3 \cdot v_N$ parameters.

The identification of the best positions of the virtual sensors is an optimization problem on a parameter vector Θ with size $2 \cdot v_N$ for the sensors' x_v and y_v coordinates. The remaining predicted values p_v can be calculated by Ordinary Kriging with x_v, y_v and the values of the k_N closest neighbors as inputs.

Substitution of (2) and (4) into the optimization criterion for v_N virtual sensors instead of k_N real sensors results in (6). The problem is highly non-linear because the weights $\omega_{v,s}$ as well as the p_v values depend both on a matrix inversion and the non-linear variogram function.

$$\theta = \begin{bmatrix} x_1 & y_1 & \dots & x_{v_N} & y_{v_N} \end{bmatrix}$$
$$\theta^* = \arg\min_{\phi} \varepsilon_T(\theta, m_s) = \tag{6}$$
$$\arg\min_{\phi} \sqrt{\frac{1}{s_{Max}} \sum_{s=1}^{s_{Max}} \left(m_s - \sum_{v=1}^{v_N} \omega_{v,s}(x_v, y_v) \cdot p_v \right)^2}$$

Small deviations of the virtual positions x_v, y_v can be tolerated without significantly increasing the training error ε_T, as long as the predicted values for the virtual sensors p_v are corrected according to position offsets. See section 4B for a sensitivity analysis. Due to this fact, it is possible to achieve at quasi-optimal parameters Θ^* with a heuristic search. During an optimization loop, the parameters in Θ are optimized one-by-one.

A. Positions of the virtual sensors

For simplification, we assume a quadratic shape of the observed area. During initialization, the virtual sensors were set on a quadratic spiral with 2 turns, with a distance between the virtual sensors of the total length of the spiral divided by v_N, see figure 1 for illustration.

During the following optimization loop the x_v, y_v coordinates are adjusted one-by-one: The training error ε_T is calculated for a small shift of the selected coordinate by $\pm\Delta_{x,y}$. The new value for the selected parameter is given by the minimum of a parable through the ε_T value for the unmodified point and the two ε_T values for the shifted points. The maximum change of the selected parameter is limited to $2 \cdot \Delta_{x,y}$ to avoid instabilities.

After one optimization step for all $2 \cdot v_N$ coordinates, $\Delta_{x,y}$ is decreased by 10% and the loop is repeated for ten times. Further loops brought only marginal improvement of ε_{Ref}.

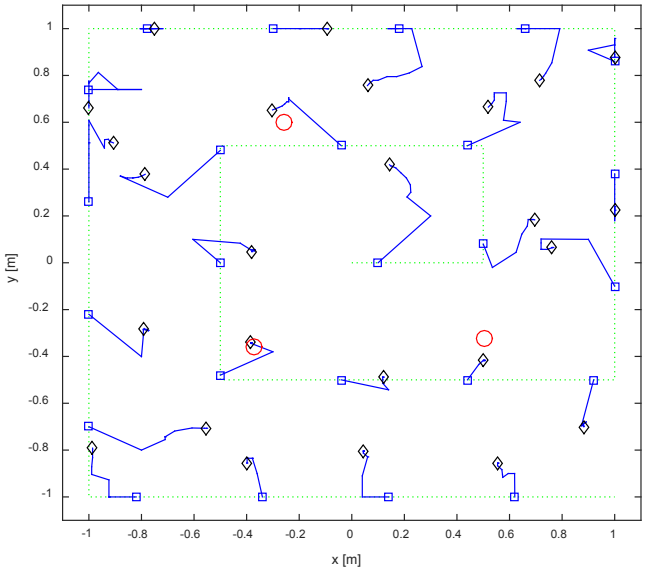

Fig. 1: Example for initial setting and optimization of the coordinates of the virtual sensors. Initial positions (blue squares) on a rectangular spiral (green doted lines). Trace of the virtual sensors during 10 optimization loops (blue lines) and final positions (blue diamonds). Maxima of the test data for a 2-diminsional field (red circles).

B. Estimation of the RBF model

As further method besides Virtual Kriging, we also evaluated the accuracy of the RBF model, which requires estimation of $4 \cdot b_{Max}+1$ parameters (7). For simplicity, we applied the same optimization process as for the virtual sensors. In addition to the coordinates x_i and y_i, also the widths λ_i and the heights a_i of each RBF function were adjusted one-by-one per optimization loop.

$$\theta_{RBF} = [c_0 \quad x_1 \quad y_1 \quad a_1 \quad \lambda_1 \quad \dots \quad x_{b_{Max}} \quad y_{b_{Max}} \quad a_{b_{Max}} \quad \lambda_{b_{Max}} \quad] \tag{7}$$

The constant offset c_0 was adjusted after each optimization step to minimize the difference between the average of the sensor measurements and the predicted field values at the same coordinates. Alternate approaches to estimate the parameters of RBF or related Green functions can be found in [4], [5], [6] and [7].

C. Test data

The test data were generated by a CFD (computational fluid dynamics) simulation of a 2-dimensional temperature field. In contrast to real measurement data from field or laboratory tests, simulated data has the advantage that full access to the undistorted field value is provided and the number and position of measurement points can be freely varied.

The simulation scenario consists of three heat sources with

a diameter of 0.4 m in a square water basin of 2m·2m size. The walls are isolated with an outside temperature of -1°C (Figure 2). Cooling is enhanced by a small flow of water with a speed of 0.01 mm/s at the inlet. Even at this low flow rate, the effect of advection was larger than that of diffusion. The influence of walls and the geometrical extent of heat sources contribute to further deviations from a simple diffusion model.

Simulations were carried out with the CFD software COMSOL. The temperature in the water basin was evaluated for 2000 randomly selected simulation points, as well as for a fixed grid of 52 by 52 points as a reference. For generating the required test data, it was sufficient to consider only the steady state. The powers of the heat sources were scaled in a way that all temperatures lay in the range between -1°C and +1°C.

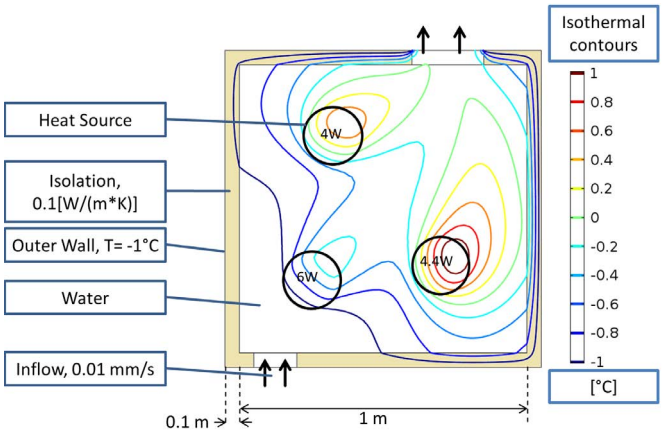

Figure 2: Setup of flow and heat transfer simulation with three heat sources inside a water basin.

The variogram for the Kriging method was estimated based on the measurement points. A good fit of the experimental variogram was achieved with a model consisting of two Gaussian functions (8), whose parameters depend on the noise RMS, e.g., n=0.009°C^2, s_1=0.0121°C^2, r_1=1.05m, s_2=0.19°C^2 and r_2=5m for σ_N=0.1°C.

$$\gamma(d) = n + (s_1 - n)\cdot\left(1 - e^{-\left(\frac{3\cdot d}{r_1}\right)^2}\right) + s_2\cdot\left(1 - e^{-\left(\frac{3\cdot d}{r_2}\right)^2}\right) \qquad (8)$$

The optimization of the position of the virtual sensors was carried out for different values of s_{Max}, σ_N and v_N. The average error of the model compared to the undistorted field ε_{Ref}, was calculated for 200 simulation runs for each parameter set. For each simulation run a new set of s_{Max} measurement points was randomly picked from the simulation data and i.i.d. noise with RMS σ_N was added. The initial step width for optimization was set to $\Delta_{x,y}$=0.1m.

The first point on the rectangular spiral was shifted by a random offset for each simulation run to avoid a bias by a fixed selection of the initialization coordinates.

IV. Simulation Results

Our simulations were centered on a standard setup with s_{Max}=200 sensors and noise RMS σ_N =0.1°C. The best possible accuracy compared with the undistorted field values was achieved with Full Kriging with a prediction error of ε_{Ref} = 0.0673°C (Table 1). Virtual Kriging achieved at almost the same error with ε_{Ref} =0.0674°C with v_N=25 virtual sensors. The error for the RBF model ε_{Ref} =0.088°C was 31% higher for b_{Max}=10 base functions.

A. *Effects of the number of sensor, noise RMS and number of virtual sensors*

Figure 3 shows the influence of the number of sensors on the prediction error. The error is for Virtual Kriging worst-case 7.8% higher than for Full Kriging at s_{Max}=500. For s_{Max}<200, Virtual Kriging achieves at an even lower error. The Virtual Kriging model has fewer degrees of freedom and thus enforces a higher smoothing of measurement noise.

The dependency of the prediction error from the noise RMS is shown in figure 4. Even under zero noise conditions, all models entail a certain minimal error, which is 2.8 times higher for Virtual Kriging than for Full Kriging. Only for σ_N≥0.1 both errors become almost the same. Virtual Kriging was in all cases better than the RBF Model.

Figure 5 shows how the error decreases with the number of virtual sensors. For v_N ≥21 hardly any difference was observed between Virtual and Full Kriging. But to be safe for variations of s_{Max} and σ_N, we selected v_N=25. The RBF model achieved at an error of 29% higher than Full Kriging with a low number of model parameters with b_{Max}=7, but almost no improvement was achieved by additional model parameters.

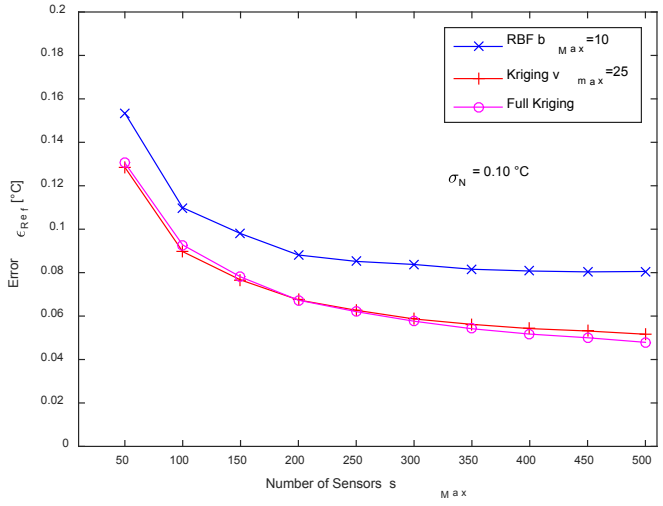

Fig. 3. Influence of the number of sensors on the prediction error for RBF and Kriging models.

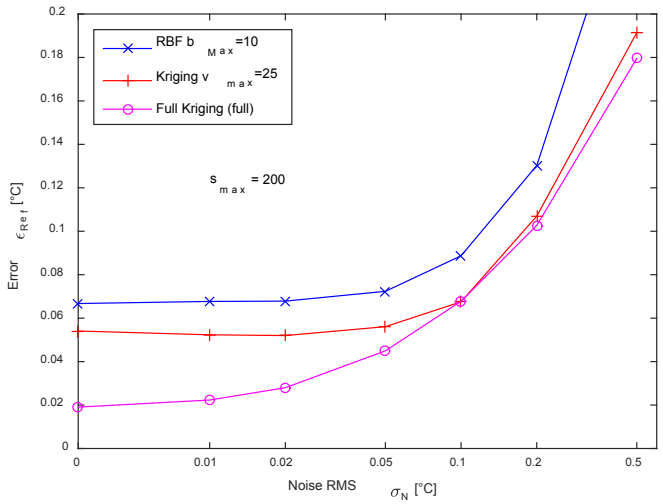

Fig. 4. Influence of noise RMS on the prediction error for RBF and Kriging models.

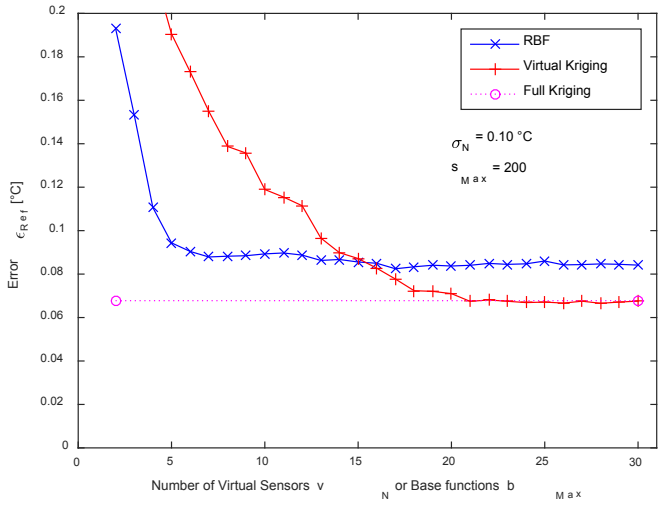

Fig. 5. Influence of model size on the prediction error for RBF and Kriging models.

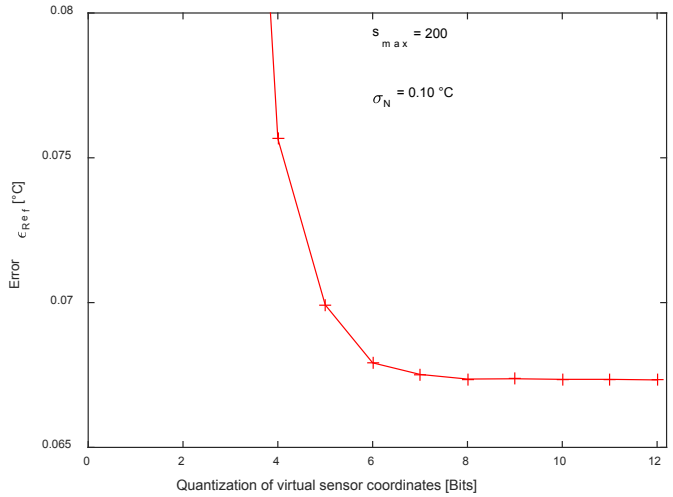

Fig. 6. Effect of quantization of the positions of the virtual sensors

B. *Quantization of virtual sensor positions*

In a final simulation, the position coordinates of the virtual sensors were rounded to different numbers of bits. The predicted value for the virtual sensor position was calculated anew after rounding. The effect of this quantization is shown in figure 6. Even with 6 bits the error is only 0.9% higher compared to field reconstruction based on floating point values for the virtual sensor coordinates. The loss of accuracy reduced to 0.04% for 8 bits.

C. *Compression rate*

Table 1 shows an example calculation of the achieved compression rate for s_{max}=200 and σ_N=0.1°C. The coordinates of the virtual sensors are less sensitive towards quantization and can be transmitted in one byte. For all other model parameters we assume two bytes. Full Kriging requires transmission of all measurement values. The variogram has to be estimated on the gateway side for Virtual Kriging, so 5 variogram parameters have to be added to the data volume. The required data volume to transmit the parameters of the two reference models and of Virtual Kriging is given in table 1. The RBF is able to compress the data volume to 20.5% compared with Full Kriging with b_{Max}=10, but at the cost of a higher prediction error. Virtual Kriging reduces the prediction error to a value similar to Full Kriging with a higher data volume of 26.25%.

Table 1: Prediction error and required number of parameters for different models.

Model	Full Kriging	Virtual Kriging	RBF model
Prediction error ε_{Ref}	0.0673	0.0674	0.088
2 Byte values	s_{max} for m_s	v_N for p_v 5 for variogram	$4 \cdot b_{max}+1$ for $p_{x,i}$, $p_{x,i}$, a_i, λ_i and c_0
1 Byte values	-	$2 \cdot v_N$ for v_x, v_y	-
Typical model size	s_{max}=200	v_N=20	b_{max}=10
Data volume	400 bytes	105 bytes	82 bytes
Relative volume	100%	26.25%	20.5%

V. Discussion

The spatial distribution of a physical quantity cannot be exactly approximated by a model with a limited number of parameters, so inaccuracies in field reconstruction cannot be avoided. But in case that the measurements are overlaid with high noise, as it is often the case in geological exploration projects for example, the error of the field reconstruction is masked by the noise.

In our simulation studies with a standard deviation of the measured temperature of ±0.422°C, there was hardly any difference between the field reconstructions based on 25 virtual sensors and by the full set of 200 real sensors if the measurement noise RMS was ≥0.1°C.

If a higher prediction error is acceptable, the measurements can be transmitted by the parameters of an RBF model. Disadvantage of the RBF model is that it cannot compensate for the higher prediction error by increasing the number of parameters. Even for 30 base functions, the error is still 25%

higher compared with Full Kriging as reference. But it has the advantage that lowering the number of parameters only slightly increased the error until a minimum of 7 base functions with an error 30% higher than of Full Kriging.

The equation of a Gaussian RBF gives only a perfect match for pure diffusion processes. Our simulations showed that the RBF model is capable to adapt to other physical phenomena such as advection by adding more base functions.

In all simulations for different numbers of sensors and measurement noise RMS values, the prediction error of Virtual Kriging was always better compared to the RFB model. Virtual Kriging should be therefore preferred for compressed transmission of the data from spatial measurements, even if the mathematical model is more complex and the required data volume was 6% higher in our test scenario.

REFERENCES

[1] Y. Wang, R. Tan, G. Xing, J. Wang, and X. Tan, "Accuracy-aware aquatic diffusion process profiling using robotic sensor networks," in *Proceedings of the 11th international conference on Information Processing in Sensor Networks*, 2012, pp. 281-292.

[2] R. Jedermann, N. Hartgenbusch, M. Borysov, C. Lloyd, U. Praeger, M. Spuler*, et al.*, "Spatial profiling of airflow conditions in cold storage warehouses by wireless anemometers," presented at the 6th International Cold Chain Management Conference, Bonn, Germany, 2016.

[3] J. McCulloch, P. McCarthy, S. M. Guru, W. Peng, D. Hugo, and A. Terhorst, "Wireless sensor network deployment for water use efficiency in irrigation," presented at the Proceedings of the workshop on Real-world wireless sensor networks, Glasgow, Scotland, 2008.

[4] I. Dokmanic, J. Ranieri, A. Chebira, and M. Vetterli, "Sensor networks for diffusion fields: Detection of sources in space and time," in *Communication, Control, and Computing (Allerton), 2011 49th Annual Allerton Conference on*, 2011, pp. 1552-1558.

[5] Y. M. Lu, P. L. Dragotti, and M. Vetterli, "Localizing Point Sources in Diffusion Fields from Spatiotemporal Samples," presented at the The 9th International Conference on Sampling Theory and Applications, Singapore, 2011.

[6] J. Murray-Bruce and P. L. Dragotti, "Estimating Localized Sources of Diffusion Fields Using Spatiotemporal Sensor Measurements," *IEEE Transactions on Signal Processing,* vol. 63, pp. 3018-3031, 2015.

[7] H. Paul and R. Jedermann, "Sparse Point Source Estimation in Sensor Networks with Gaussian Kernels," in *20th International ITG Workshop on Smart Antennas*, Munich, Germany, 2016.

[8] T. J. Hastie, R. J. Tibshirani, and J. H. Friedman, *The elements of statistical learning: data mining, inference, and prediction*, 2nd ed.: Springer, New York, 2009.

[9] R. Jedermann and W. Lang, "The minimum number of sensors - Interpolation of spatial temperature profiles," presented at the Wireless Sensor Networks, 6th European Conference, EWSN 2009, Lecture Notes in Computer Science (LNCS), Berlin/Heidelberg, 2009.

[10] M. Umer, K. L., and E. Tanin, "Spatial interpolation in wireless sensor networks: localized algorithms for variogram modeling and Kriging," *GeoInformatica,* vol. 14, pp. 101-134, 2010.

[11] D. Gu and H. Hu, "Spatial Gaussian Process Regression With Mobile Sensor Networks," *IEEE Transactions on Neural Networks and Learning Systems,* vol. 23, pp. 1279-1290, 2012.

[12] M. Jadaliha, Y. Xu, J. Choi, N. S. Johnson, and W. Li, "Gaussian Process Regression for Sensor Networks Under Localization Uncertainty," *IEEE Transactions on Signal Processing,* vol. 61, pp. 223-237, 2013.

[13] G. Reise, G. Matz, and K. Grochenig, "Distributed field reconstruction in wireless sensor networks based on hybrid shift-invariant spaces," *Signal Processing, IEEE Transactions on,* vol. 60, pp. 5426-5439, 2012.

[14] A. Agarwal, "A New Approach to Spatio-temporal Kriging and Its Applications," Ph.D. Thesis Ph.D. Thesis, The Ohio State University, 2011.

[15] H. Hu and Z. Yang, "Spatial Correlation-Based Distributed Compressed Sensing in Wireless Sensor Networks," in 2010 6th International Conference on Wireless Communications Networking and Mobile Computing (WiCOM), 2010, pp. 1-4.

[16] H. Wackernagel, *Multivariate geostatistics - an introduction with applications*. Berlin: Springer, 2003.